

## Calculated spectra for the N<sub>2</sub>–Ar van der Waals complex

By ANDRÉS GARCÍA AYLLÓN and JESÚS SANTAMARÍA

Departamento de Química-Física, Facultad de CC. Químicas,  
Universidad Complutense, 28040 Madrid, Spain

STEVEN MILLER† and JONATHAN TENNYSON†

Department of Physics and Astronomy, University College London,  
London WC1E 6BT, U.K.

(Received 4 May 1990; accepted 22 May 1990)

Calculations are presented that estimate the energies of *all* the truly bound states of the N<sub>2</sub>–Ar van der Waals complex using a semi-empirical potential-energy surface. An effective dipole surface is constructed by comparison with the infrared spectra of McKellar. These spectra are reproduced by convoluting the 30 000 strongest transitions with suitable temperature- and pressure-dependent line profiles. These synthetic spectra reproduce the observed experimental features, supporting and extending McKellar's assignments. Some of the peaks are shifted to higher frequency, suggesting that the bending potential is slightly too stiff. The corresponding 'pure' (far-infrared) spectra of the van der Waals complex are also synthesized. These do not show the low-frequency features seen in the infrared spectra.

### 1. Introduction

van der Waals systems, particularly atom–diatom complexes, have been well studied in recent years [1, 2]. For these weakly bound complexes, unlike chemically bound species, extensive potential-energy surfaces have been obtained for a number of systems by direct comparison with spectroscopic and other properties of the system [3, 4]. Although it is well known that the spectra contain information on the system not only from the transition frequencies but also from the transition intensities [5, 6], to our knowledge no attempt has yet been made to use this extra information.

Henderson and Ewing [7] obtained infrared spectra of the N<sub>2</sub>–Ar van der Waals complex by studying the simultaneous excitation of the normally infrared-inactive N<sub>2</sub> fundamental and various modes of the complex. Recently McKellar [8] has significantly improved these spectra and resolved considerable structure, which he ascribes to the van der Waals complex. These spectra were recorded at relatively high temperatures in the range 77–90 K and at several pressures. The spectra of the van der Waals complex appear as structure on the diffuse collision-induced fundamental of N<sub>2</sub>. It is these spectra that we analyse in this work.

The bound (and quasibound) rovibrational levels of N<sub>2</sub>–Ar have been studied by Brocks and van der Avoird (BvdA) [9, 10]. BvdA used the semi-empirical surface of Candori *et al.* [11], obtained from a multiproperty fit, to calculate transition frequencies and hence obtain simulated spectra. BvdA's spectra suffer from two deficiencies. First, they only considered a few rotationally excited states of the complex ( $J \leq 3$ ),

† BITNET/EARN addresses respectively: SM7 and JT at UKACRL.

and these were considered within a Coriolis-decoupling approximation. Secondly, in the absence of a reliable dipole function for the complex, BvdA assumed that all transitions involving van der Waals modes had the same intensity. Similar calculations, but using a less reliable potential-energy surface, had previously been performed by Beswick and Shapiro [12].

In this work we extend BvdA's calculations to consider *all* the truly bound states of the van der Waals complex with a variational technique that allows for the consideration of full Coriolis interactions [13, 14]. Our calculations show that the potential of Candori *et al.* supports states with  $J \leq 32$ . By guessing suitable dipole surfaces for the complex [5, 6, 15], it is possible to compute stick spectra for all the transitions involving bound states of the complex. These stick spectra are then convoluted with appropriate line profiles to give spectra that can be compared directly with McKellar's observations. By refining our effective dipole surfaces, we are able to reproduce all the features observed by McKellar that are due to truly bound states of the complex.

## 2. Calculations

### 2.1. Bound states

The bound states were obtained variationally using the potential of Candori *et al.* [11], expressed as a Legendre expansion up to  $P_8$ , and atom-diatom scattering coordinates. Since this potential is for the van der Waals coordinates only, the  $N_2$  coordinate  $r$  was frozen at  $2.0667a_0$  (equivalent to the  $N_2$  rotational constant  $B = 2.013 \text{ cm}^{-1}$  used by BvdA). Motions in the Ar- $N_2$  stretching coordinate  $R$  were represented by 40 Morse-oscillator-like functions defined by  $R_e = 11.60a_0$ ,  $D_e = 8 \times 10^{-5} \text{ au}$  and  $\omega_e = 2.2 \times 10^{-5} \text{ au}$  [16]. These functions were optimized to represent the highly bound states of the system. The angular motion  $\theta$  was carried by Legendre functions,  $P_j^k(\cos \theta)$ , with  $j \leq 11 + k$ . All calculations were performed using the TRIATOM program suite [17].

Table 1 compares our results for the vibrational levels ( $J = 0$ ) of the  $N_2$ -Ar system with those of BvdA, who used the same potential and angular basis functions as us, but numerically defined radial functions. The agreement between the two calculations is very good and suggests a high level of convergence in the results. Table 1 also gives assignments for states in terms of stretching ( $v_s$ ) and bending ( $v_b$ ) quantum numbers. These assignments were obtained by analysing plots of the wavefunctions and are substantially the same as those given by BvdA [9, 10]. However, most of the higher states are heavily mixed, and the assignments are thus somewhat arbitrary.

The assignments in table 1 are given in stretching and bending quantum numbers ( $v_s, v_b$ ). These designations are appropriate for near-harmonic states but not for states undergoing almost unhindered internal rotation, which are best described using the free-rotor model. Which model is appropriate for  $N_2$ -Ar was extensively discussed by Brocks [10], who showed that the lowest states are near-harmonic and the higher ones free-rotor-like.

Rotationally excited states of the system were obtained using the two-step procedure of Tennyson and Sutcliffe [13, 17]. The first step of these calculations neglects off-diagonal Coriolis terms by fixing  $k$ , the projection of the total angular momentum  $J$  along the body-fixed  $z$  axis, here taken to lie along the  $R$  coordinate. Coriolis-decoupled calculations for each ( $J, |k|$ ) were performed with basis sets of the same size

Table 1. Energies, relative to dissociation, of the bound states of the N<sub>2</sub>-Ar van der Waals complex with  $J = 0$ .

$v_s, v_b$	Energy/cm <sup>-1</sup>	
	Brocks [9, 10]	This work
0, 0	-77.96	-77.96
0, 1	-63.51	-63.51
1, 0	-56.19	-56.19
0, 2	-48.28	-48.29
1, 1	-46.45	-46.46
2, 0	-37.17	-37.18
0, 3	-34.96	-34.97
1, 2	-29.25	-29.26
2, 1	-27.34	-27.34
0, 4	-23.13	-23.14
3, 0	-19.79	-19.80
1, 3	-17.65	-17.66
2, 2	-12.27	-12.27
3, 1	-10.85	-10.85
4, 0	-9.64	-9.66
0, 5	-6.88	-6.89
1, 4	-5.95	-5.95
4, 1	-2.87	-2.88
5, 0	-2.86	-2.86
6, 0	-0.67	-0.65

as those described for the  $J = 0$  calculations. For  $J \geq 6$  the lowest [18]  $20J$  solutions were then used to diagonalize the fully coupled Hamiltonian. For lower  $J$  slightly larger final basis sets were used, but this had no noticeable effect on our final results.

We attempted to obtain eigenenergies and wavefunctions for all the truly bound states of the system. For  $J > 32$  we could find no bound states, although, as our calculations are variational, we cannot rigorously rule out the possibility that there may be further bound states.

In synthesising the infrared spectrum of N<sub>2</sub>-Ar, we have assumed that the bound states of the complex are independent of the vibrational state of the monomer. Studies on H<sub>2</sub>-noble-gas complexes have shown this coupling between intra- and intermolecular modes to be weak [19]. It would actually be possible to make some allowance for the effect of the N<sub>2</sub> vibrational state by using N<sub>2</sub> rotational constants appropriate to the ground and first vibrationally excited states of N<sub>2</sub>. However, these constants only differ by 0.02 cm<sup>-1</sup> and, given the errors in the van der Waals potential (see below), this correction was considered too small to be worth including.

## 2.2. Linestrengths

For all spectra discussed below the transition linestrengths were calculated using the formalism of Miller *et al.* [17, 20]. Thus the full bound-state wavefunctions from the calculations described above were used to generate transition dipoles subject only to the strict angular-momentum selection rules:

$$\left. \begin{aligned} \Delta J &= 0, & \Delta p &= \pm 1, \\ \Delta J &= \pm 1, & \Delta p &= 0, \end{aligned} \right\} \quad (1)$$

where  $p$  ( $= 0, 1$ ) is a parity quantum number such that the total parity of the system is given by  $(-1)^{J+p}$ . For van der Waals dimers this parity is more commonly given, in space-fixed coordinates, by  $(-1)^{J+l}$  (see e.g. [19]).

Given the linestrength of a transition,  $S(' \leftarrow ')$ , the contribution to the integrated absorption intensity for that transition is

$$I(\omega_0) = \frac{8\pi^3 \omega_0 g'' [\exp(-E''/kT) - \exp(-E'/kT)]}{3hQc} S(' \leftarrow '), \quad (2)$$

where the transition is of frequency  $\omega_0$  ( $= E' - E''$ ) and  $g''$  is the (nuclear-spin) degeneracy of the initial state. For transitions involving van der Waals modes *and* the  $N_2$  fundamental, the frequency factor is approximately constant and the simulated-emission Boltzmann term for the final state is effectively zero at temperatures at which the complex forms. This is in contrast with transitions between van der Waals modes *only* where these factors tend to discriminate against low-frequency transitions.

The problem with synthesizing spectra for the  $N_2$ -Ar system is that the dipole surface for the complex is not known. Thus Beswick and Shapiro [12] assumed that the dipole function was due entirely to short-range interactions. In contrast, for their simulation of the  $(N_2)_2$  dimer infrared spectrum [15] Brocks and van der Avoird (BvdA) employed a dipole surface constructed from slightly damped long-range interactions. Similar surfaces have been proposed for complexes involving  $H_2$  and noble gases [5, 6]. Despite this, in their work on  $N_2$ -Ar, BvdA assumed that all transitions had the same intensity.

Here we have followed other workers [5, 6, 15] and expanded the leading short- and long-range terms in the dipole function using (associated) Legendre polynomials. This gives a dipole function for a body-fixed axis system lying in the  $(x, z)$  plane with  $z$  along  $R$  as

$$\begin{aligned} \mu_z(R, \theta) = & \left( D_{01} e^{-(R-\sigma)/\rho} + \frac{D_7}{R^7} \right) P_0^0(\cos \theta) \\ & + \left[ \left( \frac{3}{5} \right)^{1/2} D_{23} e^{-(R-\sigma)/\rho} + \left( \frac{9}{5} \right)^{1/2} \frac{Q\alpha}{R^4} \right] P_2^0(\cos \theta) + \frac{5}{3} \frac{\Phi\alpha}{R^6} P_4^0(\cos \theta), \end{aligned} \quad (3)$$

$$\begin{aligned} \mu_x(R, \theta) = & - \left[ \left( \frac{1}{5} \right)^{1/2} D_{23} e^{-(R-\sigma)/\rho} + \left( \frac{3}{5} \right)^{1/2} \frac{Q\alpha}{R^4} \right] P_2^1(\cos \theta) \\ & - \left( \frac{10}{9} \right)^{1/2} \frac{\Phi\alpha}{R^6} P_4^1(\cos \theta), \end{aligned} \quad (4)$$

where  $\alpha$  is the polarizability of Ar,  $Q$  and  $\Phi$  are the  $N_2$  quadrupole and hexadecapole moments respectively,  $D_7$  is the dispersion induced dipole,  $\sigma$  is the size of the van der Waals complex and  $\rho$  is a range parameter. Only the two leading short-range terms are retained in this expansion, and for simplicity  $\sigma$  and  $\rho$  are assumed to be independent of  $\theta$ . The constant factors scaling the terms in (3) and (4) arise from the transformation from space-fixed to body-fixed coordinates [2].

Above, no explicit dependence of the dipole on the  $N_2$  vibrational coordinate  $r$  is given. Of course, the  $N_2$  moments ( $Q$  and  $\Phi$ ) as well as the short-range pre-exponential parameters ( $D_{01}$  and  $D_{23}$ ) all depend implicitly on  $r$ . When considering transitions

involving van der Waals modes only, to a very good approximation  $r$  can be considered as frozen. However, if a simultaneous vibrational excitation of the N<sub>2</sub> monomer is involved then it is necessary to consider the appropriately scaled derivative with respect to  $r$  of all these parameters [15].

*Ab initio* estimates of  $Q$ ,  $\Phi$ ,  $(dQ/dr)_e$  and  $(d\Phi/dr)_e$  have been given by Amos [21]. The polarizability of Ar,  $\alpha$ , is also well known [22]. Since all other terms in our dipole expansion have to be estimated or fitted to known data, our first attempt to reproduce McKellar's infrared N<sub>2</sub>-Ar spectra [8] used only the quadrupole and hexadecapole terms (see figure 1). This synthetic spectrum gave features very similar to the observed spectra in the region 15–40 cm<sup>-1</sup> above the N<sub>2</sub> fundamental. We found, as suggested by McKellar, that the major features in this region were the supposition of very many Q-branch transitions of the whole complex arising from the excitation of N<sub>2</sub> rotations within the complex.

This synthetic spectrum, however, did not reproduce the observed features in the region of the N<sub>2</sub> fundamental. In order to reproduce this portion of the spectrum, it was necessary to consider isotropic contributions to the dipole function (see figure 1). In the absence of good estimates for the values of the parameters involved in this term, we decided to estimate the isotropic dipole function by comparing synthesized spectra with those obtained by McKellar.

Analysis of our transition data showed that, to obtain good synthetic spectra, it was necessary to retain about half of the 60 000 transitions that we computed. These transitions needed to be convoluted to yield spectra that could be directly compared with McKellar's.

### 2.3. Linewidths

The linewidth of individual transitions in the observed N<sub>2</sub>-Ar infrared spectrum arises from two main causes: instrumental resolution of 0.1 cm<sup>-1</sup> and pressure-dependent line broadening.

The collision broadening is known to give a Lorentzian profile [23]

$$\mathcal{L}(\omega - \omega_0) = \frac{1}{\pi} \frac{\delta}{(\omega - \omega_0)^2 + \delta^2}, \quad (5)$$

whose width  $\delta$  can be estimated as

$$\delta = n\bar{v}\sigma, \quad (6)$$

where  $n$  is the number of particles per unit volume and  $\bar{v}$  is the mean velocity, given by the kinetic theory of gases as

$$\bar{v} = \left( \frac{8RT}{\pi M} \right)^{1/2}, \quad (7)$$

with  $R$  the ideal-gas constant,  $T$  the temperature and  $M$  the molecular mass.

The elastic-collision cross-section  $\sigma$  can be determined experimentally, from classical-trajectory calculations or from quantum calculations. For N<sub>2</sub>-Ar we have estimated the collision radius to be 7.03 $a_0$ , which is the approximate intermolecular distance between N<sub>2</sub> and Ar given by the potential used in the calculations [11].

The instrumental effect does not necessarily give a well-defined profile. For simplicity we took the instrumental profile to be Lorentzian. In this case the linewidth is merely the sum of the instrumental and collisional widths. Calculated linewidths of 0.20 and 0.38 cm<sup>-1</sup> were used to represent McKellar's experimental conditions at  $T = 77$  K,  $n = 1.7$  amagat and  $T = 87$  K,  $n = 4.4$  amagat respectively.

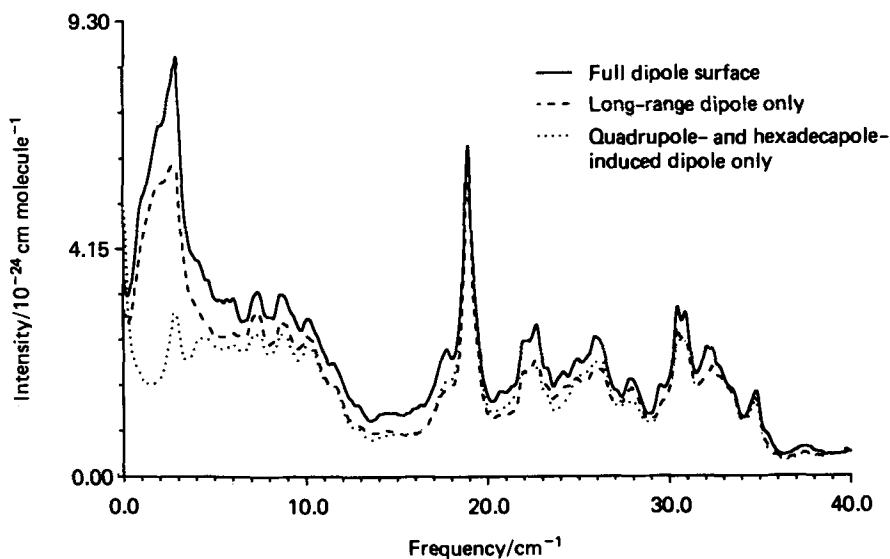


Figure 1. Comparison of simulated spectra generated using three different models for the dipole surfaces, parameters for which are given in table 2. All spectra are for a temperature of 77 K and density of 1.7 amagat. Frequencies are relative to the  $N_2$  fundamental.

### 3. Results

Once the wavefunctions for all the bound states of the  $N_2$ -Ar complex were obtained, the next stage in the calculation was to compute full infrared spectra and compare these with experiment. This was done for a number of plausible dipole surfaces. Further tests were made by comparing linestrengths for a few typical transitions, although this procedure, which is desirable since it is quicker and computationally cheaper, was found to be unreliable.

Figure 1 shows results obtained employing three different model dipole surfaces. The simplest model used only the quadrupole and hexadecapole terms, which are known accurately. This calculation was found to give spectra similar to McKellar's in the 15–40  $cm^{-1}$  region (frequencies relative to the  $N_2$  fundamental), but not to yield the observed structure in the low-frequency shift region. In particular, these calculations gave a spike at zero frequency shift, which was not observed in any of the experimental spectra. Numerical experiments showed that it was not possible to remove this structure without including isotropic terms in the dipole.

At long range the leading contribution to the isotropic dipole is given by the dispersion interaction and behaves as  $R^{-7}$ . Several values of dipole dispersion coefficient  $D_7$  were tested. It was found that only with a limited range of  $D_7$  values was it possible to suppress the zero-frequency spike. With these values the 3  $cm^{-1}$  region gained some intensity, but was still weak when compared with the observed spectra (see figure 1). It was therefore decided to investigate the effect of using short-range terms to damp the long-range contributions. As it was clear that most of the structure in the observed spectra could be reproduced by the long-range contributions alone, we only considered relatively minor effects due to short-range damping. In particular, the radius of the damping terms,  $\sigma$ , was fixed at  $6.5a_0$ , approximately the radius of the zero potential, and  $\rho$  was fixed at its 'universal' values of 0.11 $\sigma$  [23].

Table 2. Coefficients of the terms in the effective dipole surface of  $N_2$ -Ar of (3) and (4). The parameters  $Q'$ ,  $\Phi$ ,  $D'_7$ ,  $D'_{01}$  and  $D'_{23}$  are first derivatives with respect to the mass-scaled  $N_2$  normal coordinate [15].

Parameter	Final value <sup>a</sup>
$Q'$	$0.0698ea_0$ [9]
$\Phi$	$0.153ea_0^3$ [9]
$\alpha$	$11.075a_0^3$ [22]
$D'_7$	$260ea_0^8$
$D'_{01}$	$2.6 \times 10^{-4}ea_0$
$D'_{23}$	$3.9 \times 10^{-4}ea_0$
$\sigma$	$6.5a_0$
$\rho$	$0.11\sigma$ [24]

$$^a a_0 = 5.291772 \times 10^{-11} \text{ m}, e = 1.602177 \times 10^{-19} \text{ C}.$$

Final parameters for our (differential) dipole surfaces are given in table 2. These are the parameters used in figure 1. Figure 2 compares our synthetic spectrum with McKellar's best spectrum, obtained at 77 K, from which he has subtracted the contribution due to collision-induced transitions of pure  $N_2$ . Figure 3 shows our spectrum at 87 K. Again this can be compared with McKellar's spectrum, but the broader linewidth means that this spectrum contains little new information.

Although the experimental spectra so far recorded [7, 8] have been in the region of the  $N_2$  fundamental, the far-infrared spectrum of  $N_2$ -Ar is also not without interest. This spectrum does not involve a vibrational transition of the  $N_2$  monomer, and therefore the appropriate dipole surfaces are averaged, not differentiated, with respect to the  $N_2$  coordinate. In this case it is known that the long-range quadrupole

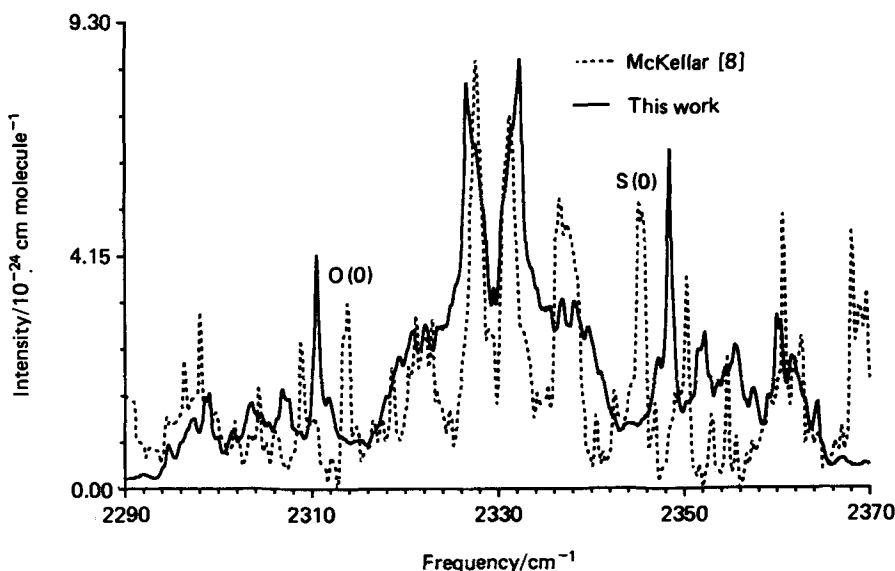


Figure 2. Comparison of the simulated spectrum for the full dipole surfaces of table 2 and (3) and (4) with the flattened experimental spectrum of McKellar [8]. Both spectra are for a temperature of 77 K and density of 1.7 amagat. The absolute intensity scale refers to the calculated spectrum only.

and hexadecapole contribution to the dipole is about 20 times larger [10, 21]. We have assumed that the other, smaller, terms in our differential surface scale in a similar fashion. This means that approximate far-infrared spectra can be generated using the same surface as that used to study the infrared region, although it should be realised that the actual intensities involved will be different because of the larger dipoles, the greatly reduced values of  $\omega$  and the effect of stimulated emission cancelling the absorption. These last two effects result in the almost complete disappearance of the low-frequency absorption features. The net result is to give spectra with similar integrated intensities.

Figures 4 and 5 give 'hot' and cold spectra of the complex in the far-infrared. For the 'hot', 77 K, spectrum we have used the same line profile to convolute the many transitions involved as that which we employed for the infrared spectrum at the same temperature. At 5 K we simply give a stick spectrum so as not to lose information.

#### 4. Discussion

The comparison of observed and calculated infrared spectra, given in figure 2, shows a number of differences. The main features of this spectrum are summarized in table 3, which also gives assignments. It should be remembered that all the features comprise many individual transitions. Indeed, the strongest transition is about a factor of 30 weaker than the strongest feature. The assignments therefore refer to Q-branch transitions (for which the total angular momentum  $J$  of the whole complex does not change) of the same internal mode, which, in McKellar's words, 'pile up' to produce sharp features on the broad spectral background.

It is not easy to assign every level for states with  $J > 3$ , owing to the overlaps of various rovibrational manifolds. The peaks, however, comprise manifolds whose strongest transitions are between  $J = 11$  and  $J = 27$ . Assignment of the features was therefore made by examining the quantum numbers of individual transitions and

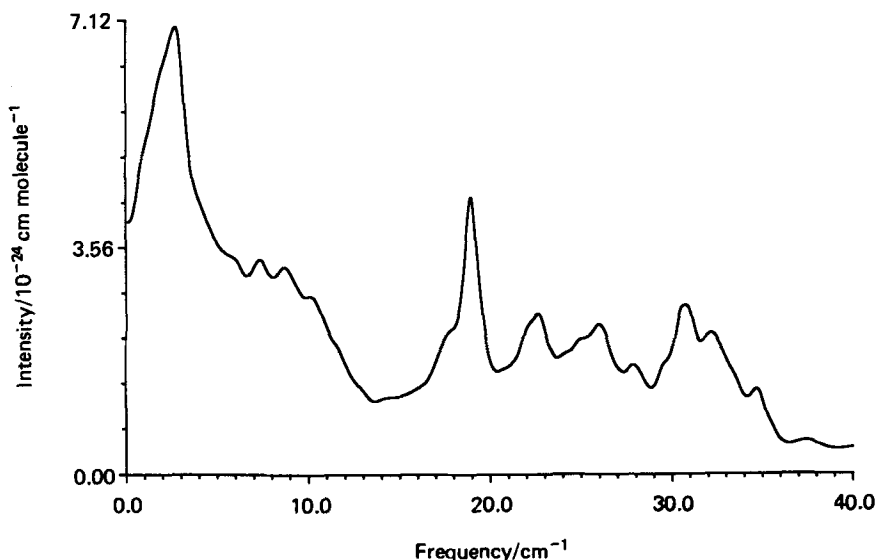


Figure 3. Simulated spectrum for the full dipole surfaces of table 2 and (3) and (4) for a temperature of 87 K and density of 4.4 amagat. Frequencies are relative to the N<sub>2</sub> fundamental.

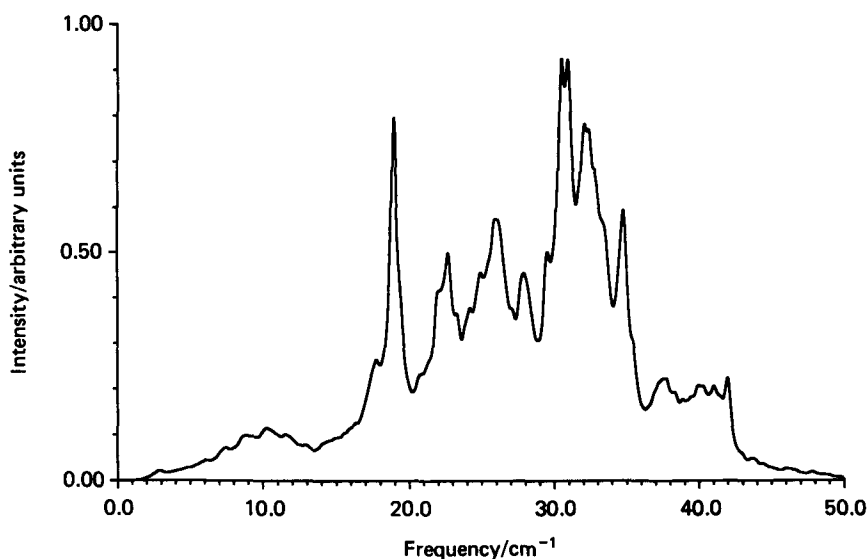


Figure 4. Simulated far-infrared spectrum for the full dipole surfaces of table 2 and (3) and (4) for a temperature of 77 K and density 4.4 amagat.

attempting to follow the members of the series to sufficiently low values of  $J$  for the rovibrational manifold to be determined.

The notation used in table 3 is consistent with that adopted by McKellar in identifying regions in his spectrum where  $N_2$  monomer transitions might occur. The notation is based on the free-rotor model. Hence  $S(n)$  and  $O(n)$  refer to transitions involving changes in the  $N_2$  angular momentum  $j$  of  $\pm 2$ .  $Q(n)$  refers to  $\Delta j = 0$  transitions. In all cases  $n$  gives the value of  $j$  in the lower state.

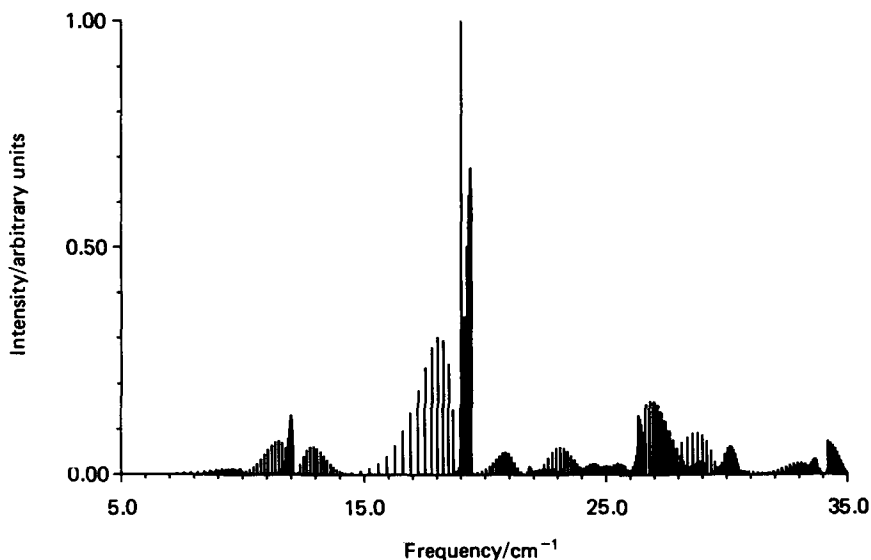


Figure 5. Simulated far-infrared stick spectrum for the full dipole surfaces of table 2 and (3) and (4) for a temperature of 5 K.

Table 3. Comparison of the main features of the blue-shifted N<sub>2</sub>-Ar infrared spectrum. All frequencies are relative to the N<sub>2</sub> fundamental. All features are Q-branch (i.e.  $\Delta J = 0$ ), except pure rotational transitions in the 0.7–3.0 cm<sup>-1</sup> region, which are R-branch transitions.

Experimental [8]/cm <sup>-1</sup>	Calculated/cm <sup>-1</sup>	N <sub>2</sub> transition	Assignment	$J_{\max}^a$
1.8	0–0.7	Q(0)	Q branch, pure rotation	Various
	0.7–3.0	Q(0)	R branch, pure rotation	Various
	3.0	O(2)	$\nu_s \leftarrow \nu_b$ difference band	11
7.5	7.6	Q(2)	$l = J \leftarrow J - 1$	17
	8.0	Q(2)	$l = J + 2 \leftarrow J + 1$	21
11.0	11.0	Q(2)	$l = 3 \leftarrow 0$	27
	11.1	Q(1)	$l = J \leftarrow J - 1$	18
	11.2	Q(1)	$l = J \leftarrow J + 1$	16
15.7	18.9	S(0)	$l = J + 1 \leftarrow J$	18
20.8	22.3	S(1)	$l = J + 2 \leftarrow J + 1$	17
25.1	25.4	S(2)	$l = J + 3 \leftarrow J + 2$	11
31.2	30.9	S(2)	$l = J + 1 \leftarrow J$	15
33.2	32.4	U(0)	$3\nu_b \leftarrow \nu_s$ difference band	12

<sup>a</sup>Value of  $J$  with the largest contribution to the manifold.

The differences between the observed and calculated spectra arise from a number of sources. Firstly some of the peaks, particularly those labelled O(0) and S(0) in figure 3, are shifted in our spectra. This must be attributed to defects in the potential of Candori *et al.* [11], which appears to be somewhat too stiff for the bending mode in the region of the minimum. The much better coincidence of the S(1) and S(2) peaks suggests that this is less of a problem away from the minimum.

Secondly, in the region about the N<sub>2</sub> band origin there is a marked difference in the shape of the absorption features. Thus what appears as an intense peak on the flattened experimental spectrum 7.5 cm<sup>-1</sup> from the band centre appears as structure on a broad feature in our calculations. We suspect that much of this difference is actually an artefact of the way McKellar separated the spectra due to the N<sub>2</sub>-Ar dimer from that due to the collision-induced spectrum of N<sub>2</sub>. The calculations clearly indicate the presence of a dense set of effectively continuous N<sub>2</sub>-Ar absorptions in this region, which McKellar's 'by-eye' reduction technique would have attributed to the continuum. This reduction technique also appears to have made the spectrum too asymmetric in the region of the band centre.

Thirdly, our calculations only considered truly bound states. McKellar's spectra cover the frequency range 2250–2450 cm<sup>-1</sup> [8]. He observed structure assignable to the N<sub>2</sub>-Ar complex over most of this frequency range. BvdA's calculations showed a regular progression of features spaced by the N<sub>2</sub> monomer rotational spacing [9, 10]. Above 40 cm<sup>-1</sup> these features were only obtained by including quasibound states in the calculation. It seems likely that quasibound states will also contribute to transitions in the S(2) and O(2) regions, which explains our underestimate of the intensity of these features.

Table 3 summarizes the main features in the spectrum of figure 2. The series of largely Q-branch transitions assigned there are by no means the only transitions in the spectrum, but are responsible for the main features. The many other transitions in the spectrum contribute largely to a quasicontinuum upon which the Q branches are

superimposed. Table 3 also gives values of  $J$  for which the integrated absorption coefficient is largest for each feature. It is notable that for all features  $J_{\max}$  is greater than 10.

Table 3 does not contain any feature associated with the stretching fundamental  $\nu_s$ . However, there is a feature that can be associated with the lowest bend-to-stretch difference band. The transition at  $32.4\text{ cm}^{-1}$  also appears to be approximated best by assignment to a difference band ( $\nu_s = 0, \nu_b = 3 \leftarrow \nu_s = 1, \nu_b = 0$  in harmonic-oscillator notation). As stretching bands are usually weak for neutral van der Waals complexes, the intensity of these transitions is almost certainly due to intensity stealing.

The differences between the infrared spectrum of figure 2 and the far-infrared spectrum of figure 4 can be understood entirely in terms of removal of the  $N_2$  vibrational frequency from the terms scaling the linestrength in the integrated intensity (2). In the far-infrared spectrum this has the effect of suppressing the low-frequency and emphasizing the higher-frequency transitions.

The low-temperature far-infrared spectrum (figure 5) shows a number of transitions with clearly resolved P, Q and R branches. The main feature is associated with the  $S(0)$  transition of the  $N_2$  monomer, which can also be thought of as the bending fundamental in the harmonic-oscillator model. The R branch for this transition has a congested bandhead that could easily be mistaken for a Q branch in a poorly resolved spectrum.

## 5. Conclusions

We have synthesised spectra involving all the truly bound states of the  $N_2$ -Ar van der Waals complex using the semi-empirical potential of Candori *et al.* [11]. This work involved computing 2759 bound energy levels, and about 60 000 transitions for each dipole surface. We are happy to supply data on transition frequencies and line-strengths to anyone who requires it. Please contact S.M. or J.T. directly.

By comparing our spectra with those observed by McKellar [8], we have been able to construct an effective dipole surface for this complex. By comparing the observed and calculated spectra, we have been able to assign many of the features in the empirical spectra lying within  $35\text{ cm}^{-1}$  of the band centre.

Features further from the band centre than this are associated with quasibound states of the complex [9, 10]. Work is currently in progress on extending our programs to quasibound states using a flux operator proposed by Miller *et al.* [25] and recently applied to van der Waals systems by Choi and Light [26]. With these states, we shall be able to synthesize the entire infrared spectrum of the  $N_2$ -Ar complex.

We wish to thank Dr A.R.W. McKellar for drawing this problem to our attention and supplying digital representations of his spectra. He and Dr Jeremy Hutson are thanked for helpful discussions. Support of this work by the British Council Acciones Integradas 1989/90 programme and Science and Engineering Research Council Grant GR/F/14550 is gratefully acknowledged. One of us (A.G.A.) gratefully acknowledges support by a Ministerio de Educación y Ciencia-FPI scholarship during the course of this work. The calculations were performed on the Cray XMP28 of the University of London Computer Centre.

## References

- [1] HALBERSTADT, N., and JANDA, K. (editors), 1990, *Dynamics of polyatomic van der Waals complexes* (Plenum).
- [2] HUTSON, J. M., 1990, *Advances in Molecular Vibrations and Collision Dynamics*, edited by J. M. Bowman (in press).
- [3] HUTSON, J. M., and LE ROY, R. J., 1985, *J. chem. Phys.*, **83**, 1197.
- [4] HUTSON, J. M., 1989a, *J. chem. Phys.*, **91**, 4448; 1989b, *Ibid.*, **91**, 4455.
- [5] DUNKER, A. M., and GORDAN, R. G., 1978, *J. chem. Phys.*, **68**, 700.
- [6] HUTSON, J. M., 1986, *Faraday Discuss. chem. Soc.*, **82**, 292.
- [7] HENDERSON, G., and EWING, G. E., 1974, *Molec. Phys.*, **27**, 903.
- [8] MCKELLAR, A. R. W., 1988, *J. chem. Phys.*, **88**, 4190.
- [9] BROCKS, G., and VAN DER AVOIRD, A., 1987, *Structure and Dynamics of Weakly Bound Molecular Complexes*, edited by A. Weber (Reidel), p. 337.
- [10] BROCKS, G., 1988, *J. chem. Phys.*, **88**, 578.
- [11] CANDORI, R., PIRANI, F., and VECCHIOCATTIVI, F., 1983, *Chem. Phys. Lett.*, **102**, 412.
- [12] BESWICK, J. A., and SHAPIRO, M., 1982, *Chem. Phys.*, **64**, 333.
- [13] TENNYSON, J., and SUTCLIFFE, B. T., 1986, *Molec. Phys.*, **58**, 1067.
- [14] TENNYSON, J., MILLER, S., and HENDERSON, J. R., 1990, *Methods in Computational Chemistry*, Vol. 5, edited by S. Wilson (Plenum).
- [15] BROCKS, G., and VAN DER AVOIRD, A., 1985, *Molec. Phys.*, **55**, 11.
- [16] TENNYSON, J., and SUTCLIFFE, B. T., 1982, *J. chem. Phys.*, **77**, 4061; 1983, *Ibid.*, **79**, 43.
- [17] TENNYSON, J., and MILLER, S., 1988, *Comput. Phys. Commun.*, **55**, 149.
- [18] SUTCLIFFE, B. T., MILLER, S., and TENNYSON, J., 1988, *Comput. Phys. Commun.*, **51**, 73.
- [19] LE ROY, R. J., and HUTSON, J. M., 1987, *J. chem. Phys.*, **86**, 837.
- [20] MILLER, S., TENNYSON, J., and SUTCLIFFE, B. T., 1989, *Molec. Phys.*, **66**, 429.
- [21] AMOS, R. D., 1980, *Molec. Phys.*, **39**, 1.
- [22] WEAST, R. C. (editor), 1988, *CRC Handbook of Chemistry and Physics* (CRC Press).
- [23] DEMTRÖDER, W., 1982, *Laser Spectroscopy* (Springer).
- [24] POLL, J. D., and HUNT, J. L., 1981, *Can. J. Phys.*, **59**, 1448.
- [25] MILLER, W. H., SCHWARTZ, S. D., and TROMP, J. W., 1983, *J. chem. Phys.*, **79**, 4889.
- [26] CHOI, S. E., and LIGHT, J. C., 1990, *J. chem. Phys.*, **92**, 2129.